The Royal Society

The hybrid effects in hybrid fibre composites: experimental study using twisted fibrous structures

By Ning Pan[1], Kezhang Chen[1]† Constantin J. Monego[2]‡ and Stanley Backer[2]

[1]*Division of Textiles and Clothing, Department of Biological and Agricultural Engineering, University of California, Davis, CA 95616, USA*

[2]*Department of Mechanical Engineering, Massachusetts Institute of Technology, Cambridge, MA 02139, USA*

Received 20 December 1996; revised 17 June 1997; accepted 22 July 1997

Considering the difficulty of obtaining reliable experimental results on hybrid composites, a new principle termed 'twist-bonding equivalence' is proposed in this paper. By means of this theory, we have used a twisted hybrid fibre strand (a yarn) as a prototype for the composites so that the fibre–matrix bonding strength can be closely simulated by adjusting the twist on the strand. Using a previously established theoretical model for hybrid composites and incorporating the properties of the strand, we have predicted results reflecting the hybrid effects. The predictions are then compared with experiments done with these twisted strands to validate the theoretical model developed for hybrid composites. Some important factors and limitations of the technique based on the 'twist-bonding equivalence' are revealed and discussed.

Keywords: composites; hybrid effects; experimental verification; twist-bonding equivalence; Weibull distribution

1. Introduction

The study of hybrid composite has become an active area in composite material research in the past few decades (Bader & Manders 1981; Bunsell & Harris 1974; Fariborz *et al.* 1985; Fukunaga & Chou 1984; Harlow 1983; Manders & Bader 1981; Marom *et al.* 1978; Phillips 1976; Qiu & Schwartz 1993; Zweben 1977). One critical issue in dealing with hybrid composites is the so-called 'hybrid effect' which is defined in Marom *et al.* (1978) as the deviation of behaviour of a hybrid structure from the 'rule of mixtures'. A positive hybrid effect means that the property is above the prediction given by the rule of mixtures, whereas a negative hybrid effect means the property is below the prediction. There is a second definition for the hybrid effect, i.e. the difference between the performance of a fibre in a hybrid composite and in a non-hybrid composite (Bader & Manders 1981; Harlow 1983). Again the hybrid effect can be positive or negative depending on whether the property in the hybrid composite is greater or smaller than that in the non-hybrid composite.

† Present address: Department of Mechanical Engineering, University of Hong Kong, Pokfulam Road, Hong Kong.

‡ Deceased.

For a hybrid composite formed by two types of fibres, the fibre type with lower breaking elongation is often termed as the LE fibre and the other type with higher breaking elongation is designated as the HE fibre. Also, there can be three different ways to define and study the hybrid effects. First, we can compare the properties of a hybrid composite with the properties of fibres from which the composite is formed. Further, we can treat the fibres collectively as a fibre bundle whose properties are well known to be different from those of the fibres. Finally, we can compare properties of a hybrid composite with properties of two non-hybrid composites, one containing the LE fibre type only, and the other containing the HE fibre type only. The conclusions drawn from the different comparisons are diverse, and great attention has to be paid when applying these conclusions.

In a previous paper (Pan & Postle 1996), three physical mechanisms have been identified and demonstrated to be responsible for causing the hybrid effects in a hybrid composite. The first (mechanism I) is the protection or enhancement afforded by the matrix to the fibres through the fragmentation process during composite extension. This enhancement effect is largely dependent on the along-fibre property variation (variation along a fibre length) and on the fibre–matrix interfacial shear strength. Because of this enhancement, the (*in situ*) behaviour of the fibres in a composite will be different from the original (*ex situ*) fibre behaviour determined before the fibres being embedded into matrix. The second mechanism (mechanism II) is related to the between-fibre property variation, i.e. variation of breaking strains between fibres of the same type. Because of this variation, fibres of the same type in the composite will break gradually according to the statistical distribution of their breaking strength or strain, eventually reducing the values of strength and breaking elongation of the composite due to the fibre–fibre interaction of the same type. Since the along-fibre property variation and the between-fibre property variation exist in both hybrid and non-hybrid composites, mechanisms I and II are also effective in a composite of single fibre type.

On a typical stress–strain curve of a hybrid composite, two stress-maximums (referred to hereafter as peaks for simplicity) can be seen: one corresponding to the point prior to the failure of LE-type fibres, which is called the principal peak (Pan & Postle 1996), and the second corresponding to the HE fibre type and called the secondary peak. Note that the failure strains associated with the two peaks are often neither identical to the breaking strains of the LE and HE fibres tested in isolation from the composite because of the difference between the fibre *ex situ* and *in situ* properties, nor identical to the breaking strains of the composites made of single fibre type of LE and HE fibres, respectively, because of the hybrid effects.

The third mechanism (III) is the cross coupling effects between the LE and HE fibres; this mechanism was found (Pan & Postle 1996), in general, to enhance the fibre *in situ* properties of LE fibre type but depresses those of the HE fibre type, leading to a positive hybrid effect associated with the principal peak and a negative hybrid effect associated with the secondary peak, when compared with non-hybrid composites.

It was also demonstrated in Pan & Postle (1996) that, of the three mechanisms, mechanism I is the main factor causing a positive hybrid effect in both breaking stress and strain by enhancing the *in situ* fibre properties. Mechanism II is responsible for the occurrence of a negative hybrid effect when the composite is compared with single fibres. When comparing a composite with a fibre bundle, however, the effect due to mechanism II will be eliminated since the between-fibre property variation is effective

in both cases. Mechanism III, as mentioned above, causes positive hybrid effects in the principal quantities, but negative hybrid effects in the secondary quantities.

As stated before, since mechanisms I and II exist even in a non-hybrid composite, the effects associated with these two mechanisms will also occur in such composites. Therefore a more rational definition for a genuine hybrid effect which should only be found in a hybrid composite is the one addressing the influence caused by the cross-coupling effect between different fibre types, i.e. the influence associated with mechanism III. This cross-coupling effect can only be detected by comparing the properties of the hybrid composite with a single-fibre-type composite.

The effects of the three mechanisms were shown in Pan & Postle (1996) to be strongly dependent on the key variables involved, including the hybrid ratio for fibre LE, the system fibre volume fraction, the shear yielding strength of the fibre–matrix interface and the fibre tensile modulus ratio between the LE and HE types.

Experimental verification of the theoretical predictions on hybrid composite behaviour is, however, extremely difficult. Even for a non-hybrid fibre composite, because of the existence of various defects, statistical variations and perturbations in the fibre–matrix interface, and in the properties of the constituents and in the composite structure, the real composite specimens differ significantly from the ideal theoretical models established based on many necessary but often unrealistic assumptions. Consequently, in most cases, experimental results obtained from the composite specimens are unable to provide accurate and reliable information to validate the theoretical models.

To reduce the experimental errors caused by irregularities in composite specimens, one approach is to adopt the so-called microcomposite as an experimental model, used as early as in 1971 by Aveston (1971). The microcomposite is a composite made of a single or a few fibres embedded in matrix. Because at most there are only a few fibres, they can be carefully selected, accurately positioned in and securely bonded with the matrix to minimize the irregularities so as to make it closer to an ideal experimental specimen. This idea has since become widely accepted and used (Andersons & Tamuzs 1993; Andrews & Young 1995; Baxevanakis *et al.* 1994; Curtin 1991*a*, *b*; Curtin *et al.* 1994; Goda *et al.* 1995; Ho *et al.* 1995; Houpert *et al.* 1994; Kushnevsk *et al.* 1994; Netravali *et al.* 1989; Park *et al.* 1994; Shioya & Takaku 1978; Venkatakrishnaiah & Dharani 1993; Wagner & Eitan 1990; Wagner *et al.* 1991; Watson & Clyne 1992; Yavin *et al.* 1991).

Although this method has eliminated some of the error sources, there are still problems. First, the effects associated with the between-fibre variation cannot be studied by using the microcomposite, owing to the fact that there is only one or a few fibres in the specimen. Even though useful information about the real composite system can be obtained by examining the microcomposite, there also exists a size or scale effect when one attempts to predict the system properties based on the conclusion scaled up from a microcomposite. More importantly, no matter how elaborately the microcomposite is prepared, there are still certain variables either unknown or difficult to control, such as, notoriously, the bonding properties between fibre and the matrix. Several factors are attributable to this latter problem. First, our understanding of the bonding process during composite manufacturing and the nature of the fibre–matrix bond is still not adequate for us to predict the bonding strength with reasonable accuracy. Many therefore have questioned the rationality of using the interfacial strength as an indicator for bonding quality between fibre and the matrix (Hsueh 1992; Karbhari & Engineer 1995; Kodokian & Kinloch 1989;

Wagner & Eitan 1990) Furthermore, bonding properties between fibre and matrix, even after carefully monitoring, are still subject to variations, leading to uncertainty in the fibre–matrix interface.

Phoenix has dealt extensively with both twisted fibrous structures and composites as one group of the so-called fibrous structures (Phoenix 1979*a*, *b*; Pitt & Phoenix 1981). The present authors have focused on the similarities between a fibre-reinforced composite and a twisted yarn (Pan 1992; Monego *et al.* 1994). Mechanistically, a twisted yarn can be treated as a composite where individual fibres are embedded in the matrix formed by neighbouring fibres. The only major difference between the two structures lies in the nature of the fibre–matrix bonding. In a composite, the bonding is largely chemical, whereas in a yarn it is entirely frictional. Moreover, the fragmentation phenomenon, which is the typical fibre fracture behaviour in a composite, was also observed in a yarn structure (Machida 1963; Monego 1966; Monego & Backer 1968). The two structures have so much in common that most analytical and experimental techniques are applicable to both. More recently, in a paper by two of the present authors (Monego *et al.* 1994), it is explicitly proposed that a blended filament strand can be used as a pseudo-hybrid composite system and the effect of interfacial shear strength on the performance of a hybrid composite can be simulated by varying the twist of the strand.

In this paper, we shall further develop the concept that a twisted yarn can be used as an experimental model for composite study. We shall first establish the twist and bond relationship, termed the 'twist-bonding equivalence', in this paper so that by altering the twist level, which is very easy to do, we can accurately control and adjust the 'bonding' properties between the fibre and the 'matrix' in a yarn. There are other additional benefits of using this model, such as ease of sample preparation and experiment observation, and better uniformity of the samples.

As an example of the application of this method, we shall use a theoretical model developed in Pan & Postle (1996) for hybrid composites, substituting in it the fibre properties provided in the experimental work on blended yarn mechanics (Monego 1966) to yield the predictions of the hybrid effects similar to those in Pan & Postle (1996). These predictions will then be compared with the experimental results to substantiate the validity of the hybrid composite model proposed in Pan & Postle (1996), and therefore the concept of the 'twist-bonding equivalence'.

2. Twist-bonding equivalence

The extent of twisting on a strand of unit length depends on two variables, i.e. the number of twist (turns) and the thickness of the yarn. The so-called yarn twist factor (T_{y}) is therefore used by the textile professionals to reflect the joint effect of the two variables, and is defined as

$$T_{\mathrm{y}} = \frac{\mathrm{tpc}}{\mathrm{tex}}, \tag{2.1}$$

where 'tpc' represents the number of twists per cm, and 'tex', termed yarn count, is defined as the weight in grams of a yarn per 1000 m long, an indirect measure of the yarn thickness to avoid the difficulty of directly measuring the yarn of extremely variable and tiny cross section.

The fibre gripping action in a twisted yarn results from the frictional force related to the transverse pressure generated by the yarn axial tension, because of the helix

arrangement of individual fibres in the yarn. Based on analyses of yarn strength (Pan 1993*a*) and composite strength (Kelly & Macmillan 1986, p. 252), we can establish the relation

$$\mu g = \tau_{\mathrm{b}}, \tag{2.2}$$

where τ_{b} is the bonding shear strength between fibre and matrix in a composite, μ is the inter-fibre frictional coefficient in a yarn, and g is the transverse pressure and can be calculated according to Pan (1992):

$$g = \frac{n}{2\mu} E_{\mathrm{f}} \epsilon_{\mathrm{y}} \eta_q, \tag{2.3}$$

where ϵ_{y} is the yarn strain, and

$$n = \sqrt{\frac{G_{TL}}{E_{\mathrm{f}}} \frac{2}{\ln 2}} \tag{2.4}$$

is an indicator of the gripping effect of the yarn structure on each individual fibre, and is dependent on the ratio of yarn shear modulus G_{TL}, governing shear in the plane of longitudinal (L) and transverse (T) directions, and fibre tensile modulus E_{f}, as well as the fibre arrangement within the yarn, reflected in the analysis of Pan (1992). η_q represents the fibre orientation effect, and is defined in Pan (1993*b*) based on the assumption of a random distribution of fibre orientation:

$$\eta_q = \frac{2q(1-\nu_{LT}) + (1+\nu_{LT})\sin 2q}{4q}, \tag{2.5}$$

where q is the helix angle at the yarn surface and can be taken as a constant for a given yarn structure and can be calculated from Hearle *et al.* (1969)

$$q = \arctan[10^{-3} T_{\mathrm{y}} \sqrt{(40\pi/\rho V_{\mathrm{f}})}], \tag{2.6}$$

where ρ and V_{f} represent the fibre density and fibre volume fraction in the yarn, and the yarn Poisson's ratio ν_{LT} governing induced strain in the T direction owing to strain in the L direction is given in Pan (1992):

$$\nu_{LT} = \frac{\sin^5 q}{2(1-\cos^3 q)(q/2 - 1/4 \sin 2q)}. \tag{2.7}$$

The shear modulus G_{TL} for a yarn consisting of continuous members can be calculated as (Pan 1992):

$$G_{TL} = \frac{E_{\mathrm{f}} V_{\mathrm{f}}}{S(T,L)}, \tag{2.8}$$

where

$$S(T,L) = \frac{\pi(1-\cos q)\sin^3 q}{6(q/2 - 1/4\sin 2q)^2} + \frac{8\sin^3 q}{3\pi(1-\cos q)(1+\cos q)^2} + \frac{\pi(4 - 3\cos q - \cos^3 q)}{6(q/2 - 1/4 \sin 2q)(1+\cos q)}. \tag{2.9}$$

Here again T and L stand for the transverse and longitudinal directions.

Substituting all the related equations into equation (2.2), a connection between the interfacial shear strength τ_{b} of a composite and the strand twist factor T_{y} is established. This relationship is a function of, among other variables, the yarn breaking

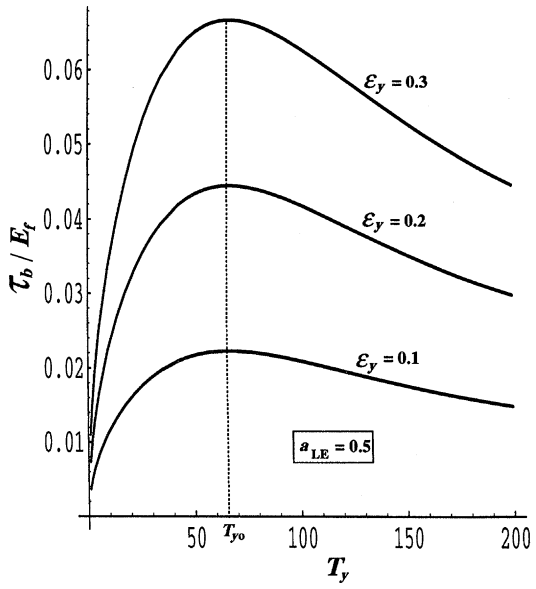

Figure 1. Twisting-bonding equivalence at three yarn breaking strain levels.

strain ϵ_y, as indicated in equation (2.3), where the transverse pressure g which generates the inter-fibre friction is directly related to ϵ_y. A plot of this τ_b, in relative scale of τ_b/E_f, and T_y relationship is shown in figure 1 at three levels of ϵ_y. First of all, it is clear that a higher ϵ_y will generate higher inter-fibre friction in a yarn, which is equivalent to a greater interfacial shear strength τ_b in a composite. Also, the increase of twist level T_y corresponds to a higher τ_b value, but up to a limit beyond which the τ_b value will decrease. This is caused by the so-called 'obliquity' effect in an over-twisted yarn, where too much twist leads to significant discrepancy between fibre orientation and the yarn axis so that the yarn strength as well as the transverse pressure are both reduced. Therefore, the applicability of this twist-bonding equivalence principle is limited up to the optimal twist level T_{yo}, as indicated in figure 1, which is a constant for a given yarn independent of the yarn strain level.

3. The theoretical model

A new theoretical treatment of stress–strain relation for a hybrid composite has been proposed by Pan & Postle (1996), which can be applied to a hybrid strand with necessary alternation as the following. When a tensile strain ϵ_y is applied to a hybrid strand with two fibre types of lower breaking elongation (LE) and higher breaking elongation (HE), the stress σ_y on the hybrid strand can be expressed as

$$\sigma_y = (a_{LE}S_{LE}\sigma_{LE} + a_{HE}S_{HE}\sigma_{HE})V_f = (a_{LE}S_{LE}\epsilon_{LE}E_{LE} + a_{HE}S_{HE}\epsilon_{HE}E_{HE})V_f, \quad (3.1)$$

where V_f is the fibre volume fraction of the strand, and for a perfectly packed strand, as in the sample employed in the experimental section below, we can readily calculate that $V_f = 0.9069$. a_{LE} and a_{HE} are called the hybrid ratios, and a_iV_f gives the volume fraction for fibre type i = LE or HE. σ_i, ϵ_i and E_i are the stress, strain and tensile modulus of the fibre types i.

Although equation (3.1) seems to resemble the 'rule of mixtures', very important modifications have been made here. First of all, S_{LE} and S_{HE} in the equation represent

the fractions of components of types LE and HE which have not yet failed at the given strain level ϵ_y, and are still carrying load; so they are termed the surviving ratios and are apparently functions of the strain ϵ_y. These two variables actually reflect the fact that due to the between-fibre variation in the breaking strain, the components of the same type will not break simultaneously at a given strain. Rather they will break over a strain span.

We assume that the breaking strain of the fibres is best described by a Weibull distribution. So for a fibre with original length l_f, the probability of the fibre breaking strain being ϵ_f can be written as

$$F(\epsilon_f) = 1 - \exp[-l_f \alpha \epsilon_f^{\beta}], \tag{3.2}$$

where α and β are the Weibull scale and shape parameters of the breaking strain distribution. Then the surviving ratio for a fibre bundle of type i = LE or HE can be expressed as

$$S_i = \exp[-l_c \alpha \epsilon_f^{\beta}], \tag{3.3}$$

where l_c is the critical fibre length. From Pan & Postle (1996) we have

$$l_c = \left[\frac{r_f(\frac{4}{3}\alpha)^{-1/\beta}\Gamma(1+(1/\beta))}{n\eta_q\epsilon_y}\right]^{\beta/(1+\beta)}, \tag{3.4}$$

where r_f is the fibre radius.

As stated in Pan & Postle (1996), we realize that the definition of the critical fibre length in equation (3.4) is an idealized result, and there are several modified models proposed (see, for example, Feillard *et al.* 1994). Yet for briefness, we still apply equation (3.4) in our analysis. For a hybrid composite where two fibres of types LE and HE are used, this critical length, like S_i, will possess different values for the two fibre types.

The principal and secondary breaking strains of the hybrid composite, associated with the first and second peaks on the stress–strain curve for a hybrid fibrous structure implicitly defined in equation (3.1), will be the strains corresponding to the maximum values of stress in equation (3.1), which can be derived by solving the equation $\mathrm{d}\sigma_y/\mathrm{d}\epsilon_y = 0$, as proposed in Pan & Postle (1996). This is the technique we have used to obtain the theoretical predictions presented in the following section.

4. The experimental results and discussion

We introduce here an early piece of experimental work done by some of the present authors (Monego 1996; Monego & Backer 1968) which provides systematic results for our purpose of verifying the theoretical predictions.

This work used mechanical tracer elements as a means of studying rupture mechanisms in continuous twisted structures of blended fibre types. To facilitate experimental control and observation, a set of fibre strands were made. Each strand consisted of 91 components, either cotton yarns (the LE components) or polyester (PET) filament yarns (HE components), drawn from independent packages in a creel and twisted carefully with negligible radial migration. The 91 components were distributed in five helical layers about a central or core yarn. A range of such model strands were prepared which varied from 0–100% for cotton composition (100–0% for polyester) with twist factor T_y ranging from about 5.0 to 45.0. In this model strand,

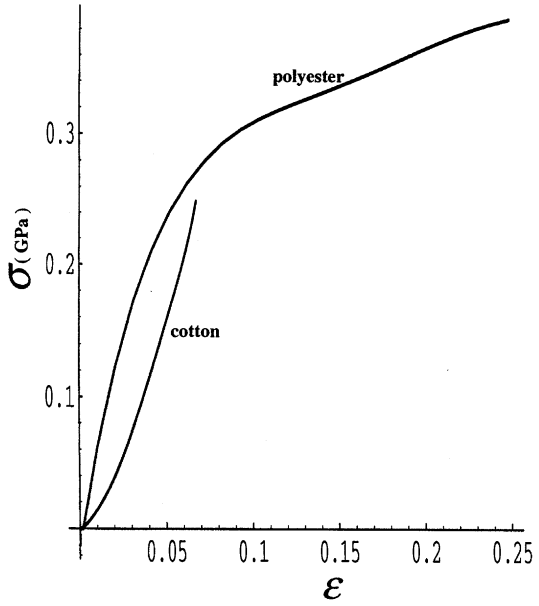

Figure 2. The stress–strain curves for the LE and HE components.

Table 1. *component properties (Monego 1966)*

item	cotton (LE)	PET (HE)	unit
yarn count	7.44	7.78	tex
radius r	41.2×10^{-4}	41.9×10^{-4}	cm
density ρ	1.54	1.38	g cm^{-3}
gauge length l_0	20.32	20.32	cm
frictional coefficient μ	0.20	0.26	
mean breaking strain $\overline{\epsilon_f}$	6.75	29.3	%
mean strength $\overline{\sigma_f}$	0.25	0.43	GPa
number N_i	$91 \times a_{\mathrm{LE}}$	$91 \times a_{\mathrm{HE}}$	
shape parameter β	8.75	44.46	
scale parameter α	5.60×10^3	5.56×10^{14}	cm^{-1} GPa$^{-\beta}$

the polyester components are yarns of 7.78 tex, formed by 34 filaments. And the cotton components are of 7.44 tex. The typical curves of the stress–strain relations for the two components are provided in figure 2, and the properties of the components can be found in table 1.

In this paper, our main objective is to verify the theoretical predictions in Pan & Postle (1996) on the hybrid effects defined there as the discrepancy between the properties of a constituent component in a hybrid and in a single-fibre-type structure. If we take breaking strain as an example, we can define two ratios, $\epsilon_{y1}/\epsilon_{y\mathrm{LE}}$ and $\epsilon_{y2}/\epsilon_{yHE}$, to specify the hybrid effects for the two components, respectively. Here $\epsilon_{y\mathrm{LE}}$ and $\epsilon_{y\mathrm{HE}}$ are the breaking strains for the two corresponding components in non-hybrid structures, whereas ϵ_{y1} and ϵ_{y2} are the breaking strains of the two components in a hybrid system, i.e. the breaking strain values corresponding to the two peaks on a stress–strain curve for the hybrid strand. If the two strain ratios, $\epsilon_{y1}/\epsilon_{y\mathrm{LE}}$ and

Table 2. *Experimental data for the ratio* $\epsilon_{y1}/\epsilon_{y\mathrm{LE}}$

a_{LE}	T_{y} =5.17	10.34	20.77	31.10	41.53
0.000	3.940	3.610	3.140	2.670	2.360
0.011	3.820	3.560	3.000	2.630	2.220
0.022	3.820	3.610	2.980	2.590	2.250
0.110	1.110	1.050	1.090	1.110	1.190
0.220	0.940	0.940	1.050	1.040	1.030
0.330	1.090	1.080	1.070	1.070	1.070
0.440	1.030	0.970	1.000	0.940	0.840
0.560	0.940	1.000	0.980	1.040	1.030
0.670	0.910	0.970	0.950	0.810	0.800
0.890	1.010	1.000	1.020	0.990	1.020
1.000	1.000	1.000	1.000	1.000	1.000

Table 3. *Experimental data for the ratio* $\epsilon_{y2}/\epsilon_{y\mathrm{HE}}$

a_{LE}	T_{y} =5.17	10.34	20.77	31.10	41.53
0.000	1.000	1.000	1.000	1.000	1.000
0.011	0.970	0.980	0.960	0.990	0.940
0.022	0.970	1.000	0.950	0.970	0.950
0.110	0.890	0.950	0.930	0.360	0.357
0.220	0.930	0.920	0.910	0.355	0.360
0.330	0.980	0.950	0.890	0.360	0.352
0.440	0.780	0.860	0.320	0.350	0.360
0.560	0.980	0.950	0.310	0.350	0.350
0.670	1.020	0.920	0.300	0.310	0.340
0.890	0.920	0.820	0.330	0.360	0.430
1.000	0.250	0.280	0.320	0.380	0.420

$\epsilon_{y2}/\epsilon_{y\mathrm{HE}}$, are greater or smaller than unity, the hybrid effect would be positive or negative, respectively.

The stress–strain curves in figure 2 for the two components have been converted into polynomial expressions using regression analysis. For each given level of yarn strain ϵ_{y}, the average fibre strain ϵ_{f} will be

$$\epsilon_{\mathrm{f}} = \eta_q \epsilon_{\mathrm{y}}, \tag{4.1}$$

where η_q is defined in equation (2.5). Bringing this fibre strain into equation (3.3), the surviving ratios for the two components, S_{LE} and S_{HE}, can be calculated and used in equation (3.1). The breaking strains ϵ_{y1} and ϵ_{y2} associated with the two peaks on the stress–strain curve can then be derived by finding the maximum stresses in equation (3.1) the same way as in Pan & Postle (1996). The breaking strains for the non-hybrid strands $\epsilon_{y\mathrm{LE}}$ and $\epsilon_{y\mathrm{HE}}$ can be obtained in similar way by setting $a_{\mathrm{LE}} = 1$ or $a_{\mathrm{LE}} = 0$ in equation (3.1), respectively.

From the experimental results, we have extracted the data for the two ratios at different levels of the hybrid fraction for the LE component, a_{LE}, and of the twist factor T_{y}. They are shown in table 2 for $\epsilon_{y1}/\epsilon_{y\mathrm{LE}}$ and in table 3 for $\epsilon_{y2}/\epsilon_{y\mathrm{HE}}$. These

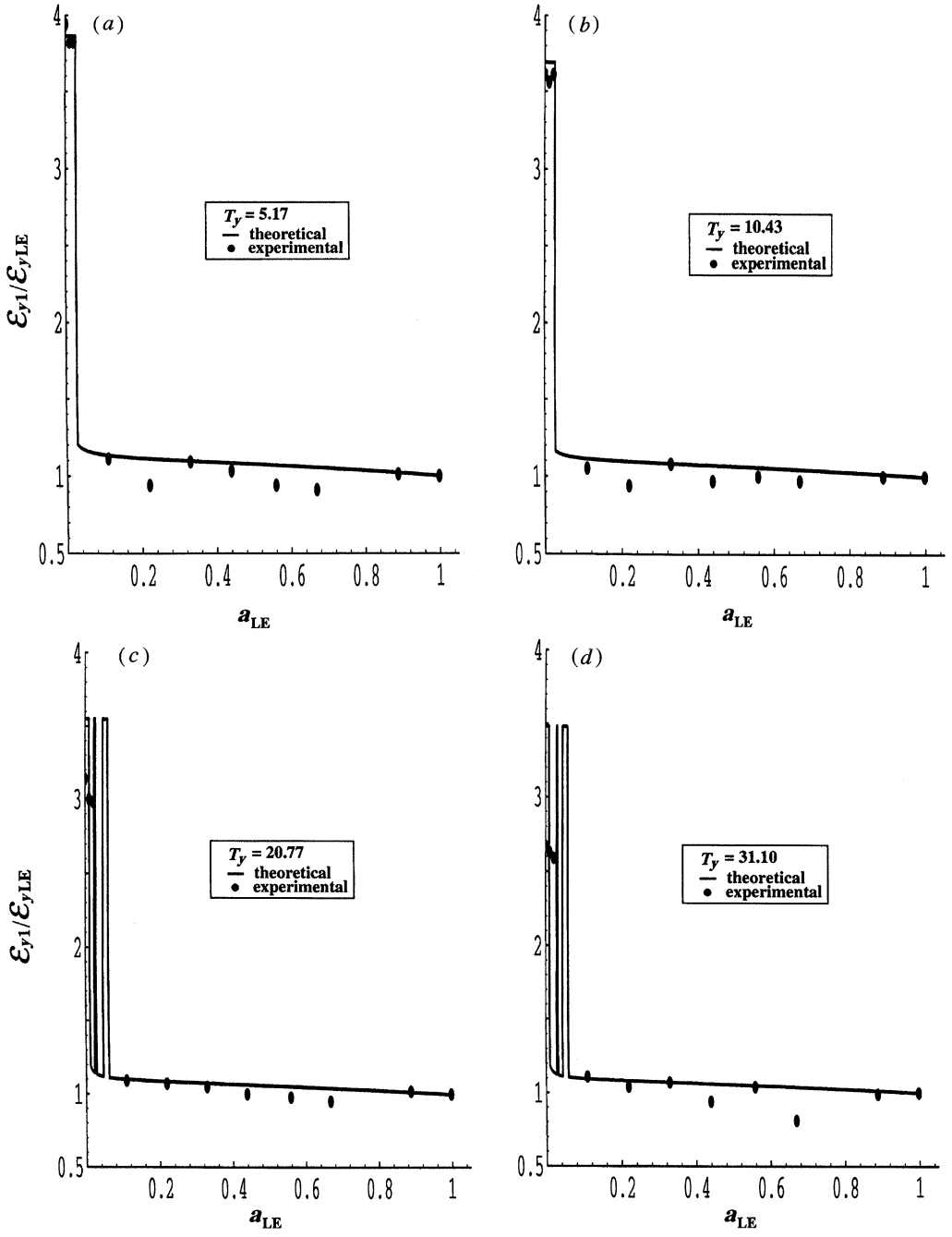

Figure 3. Comparisons between the principal breaking strain of a hybrid composite and the breaking strain of the LE fibre composite. $\epsilon_{y1}/\epsilon_{y\mathrm{LE}}$ versus the hybrid ratio a_{LE} when: (*a*) $T_{\mathrm{y}} = 5.17$; (*b*) $T_{\mathrm{y}} = 10.43$; (*c*) $T_{\mathrm{y}} = 20.77$; (*d*) $T_{\mathrm{y}} = 31.10$.

data will be used to verify the predictions from the theoretical model in equation (3.1) by using the component properties provided in table 1. The comparisons between them are provided in figures 3–6.

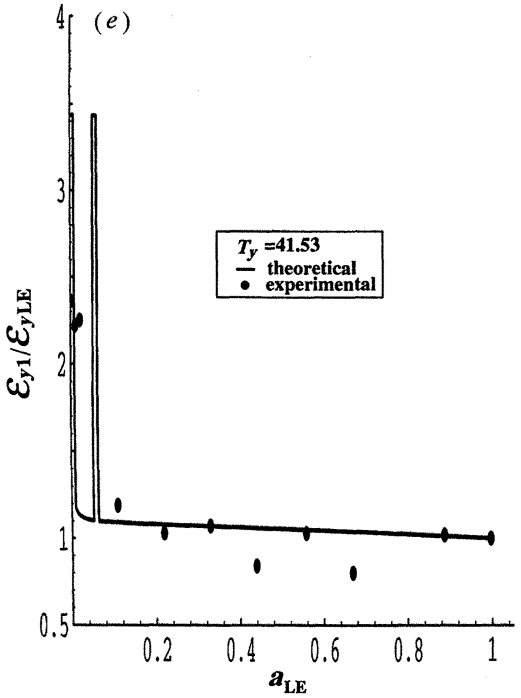

Figure 3. *Cont.* Comparisons between the principal breaking strain of a hybrid composite and the breaking strain of the LE fibre composite. $\epsilon_{y1}/\epsilon_{y\mathrm{LE}}$ versus the hybrid ratio a_{LE} when (*e*) $T_{\mathrm{y}} = 41.53$.

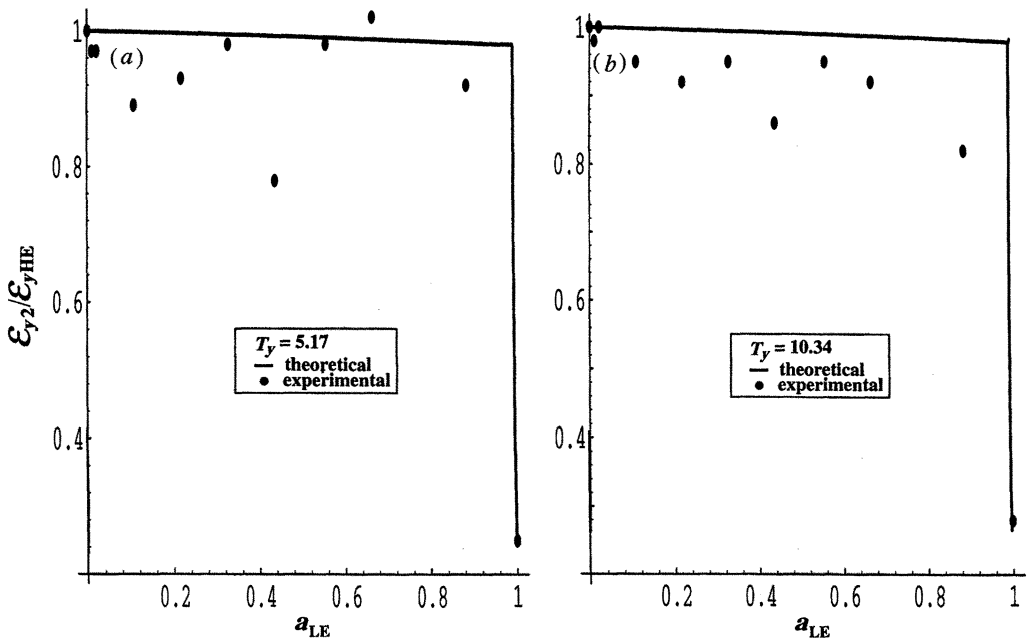

Figure 4. Comparisons between the secondary breaking strain of a hybrid composite and the breaking strain of the HE fibre composite. $\epsilon_{y2}/\epsilon_{y\mathrm{HE}}$ versus the hybrid ratio a_{LE} at: (*a*) $T_{\mathrm{y}} = 5.17$; (*b*) $T_{\mathrm{y}} = 10.43$.

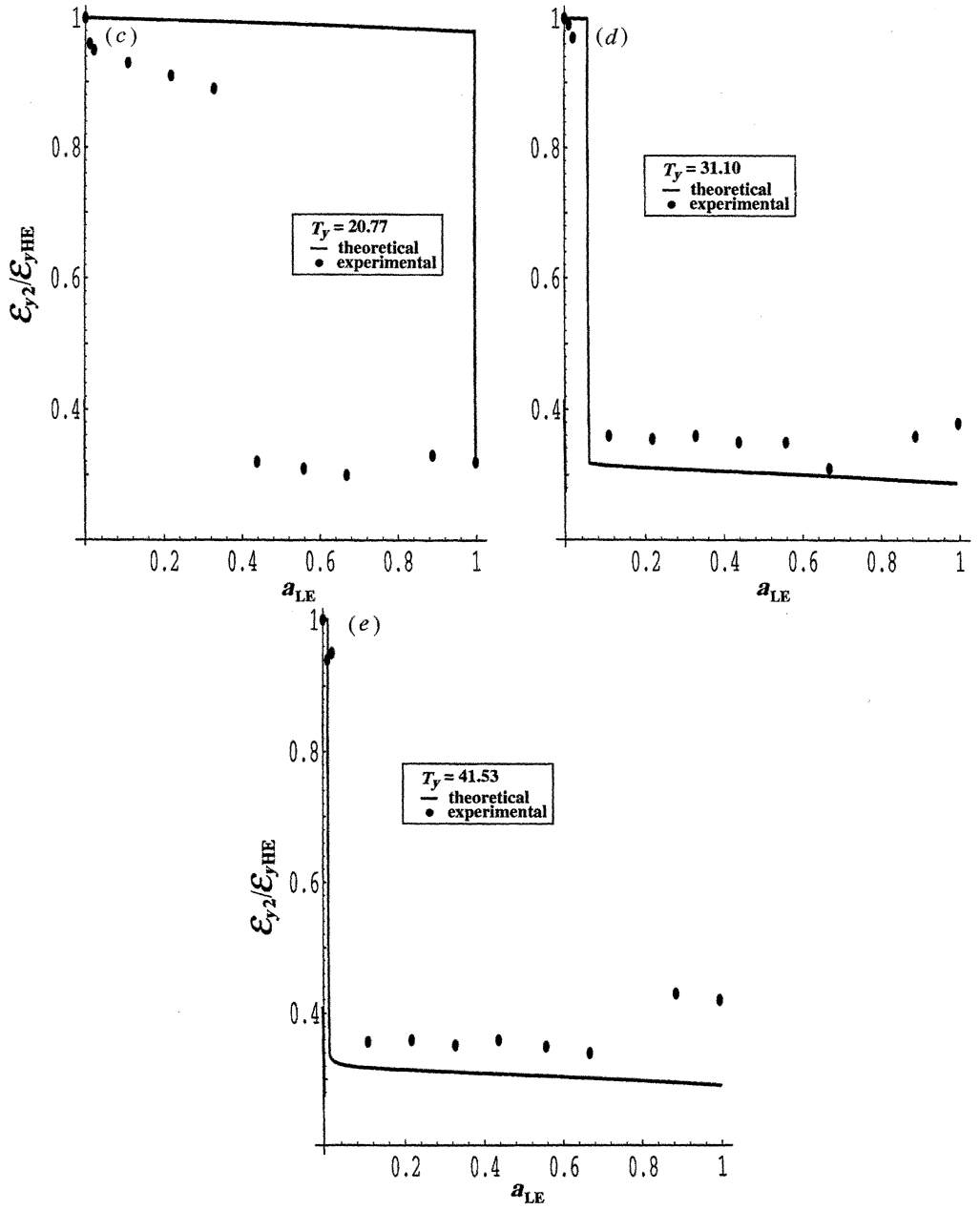

Figure 4. *Cont.* Comparisons between the secondary breaking strain of a hybrid composite and the breaking strain of the HE fibre composite. $\epsilon_{y2}/\epsilon_{y\mathrm{HE}}$ versus the hybrid ratio a_{LE} at: (*c*) $T_{\mathrm{y}} = 20.77$; (*d*) $T_{\mathrm{y}} = 31.10$; (*e*) $T_{\mathrm{y}} = 41.53$.

First of all, the results of $\epsilon_{y1}/\epsilon_{y\mathrm{LE}}$ as a function of hybrid fraction a_{LE} are illustrated in figure 3*a*–*e*, corresponding to five different levels of the twist factor from $T_{\mathrm{y}} = 5.17$–41.53. Over the twist range shown in the figures, the trends of both theoretical and experimental results are similar. When a_{LE} is small, we have $\epsilon_{y1}/\epsilon_{y\mathrm{LE}} \gg 1$ or $\epsilon_{y1} \gg \epsilon_{y\mathrm{LE}}$, meaning that there exists a significant positive hybrid effect at low a_{LE} level, similar to that reported in Fukuda *et al.* (1984) on hybrid composite. The

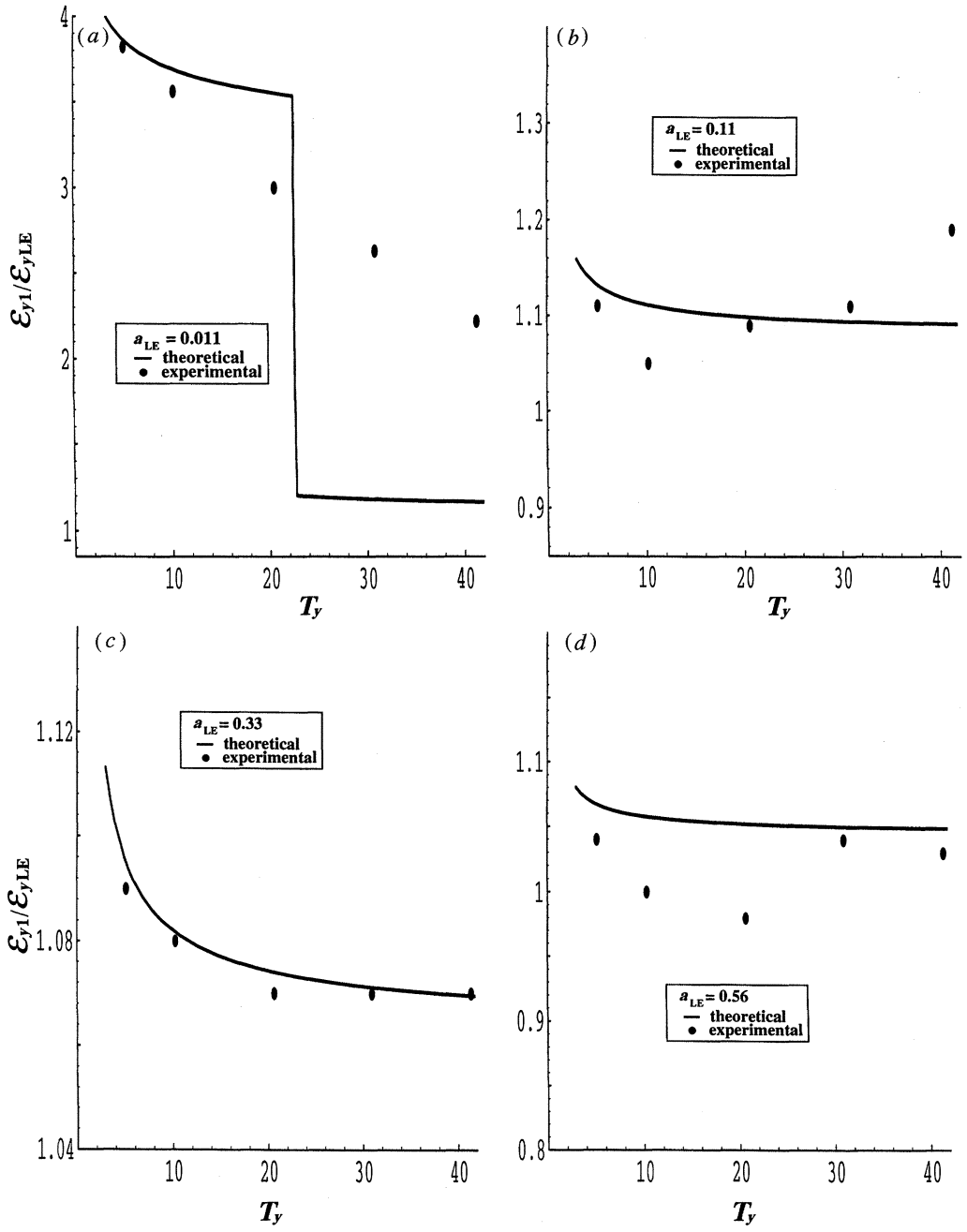

Figure 5. Comparisons between the principal breaking strain of a hybrid composite and the breaking strain of the LE fibre composite. $\epsilon_{y1}/\epsilon_{y\mathrm{LE}}$ versus the twist factor T_{y} when: (*a*) $a_{\mathrm{LE}} = 0.011$; (*b*) $a_{\mathrm{LE}} = 0.11$; (*c*) $a_{\mathrm{LE}} = 0.33$; (*d*) $a_{\mathrm{LE}} = 0.56$.

specific value of $\epsilon_{y1}/\epsilon_{y\mathrm{LE}}$ at this point, however, is affected by the twist factor T_{y}. Both theoretical predictions and experimental data, albeit having some discrepancies between them, show that the lower the T_{y} value, the greater the $\epsilon_{y1}/\epsilon_{y\mathrm{LE}}$ ratio at low a_{LE} level. As a_{LE} increases to a certain critical level which again varies depending on

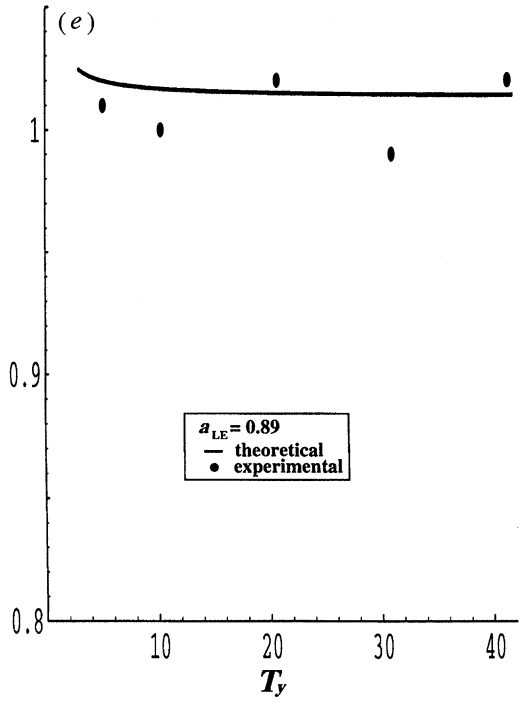

Figure 5. *Cont.* Comparisons between the principal breaking strain of a hybrid composite and the breaking strain of the LE fibre composite. $\epsilon_{y1}/\epsilon_{y\mathrm{LE}}$ versus the twist factor T_{y} when (*e*) $a_{\mathrm{LE}} = 0.89$.

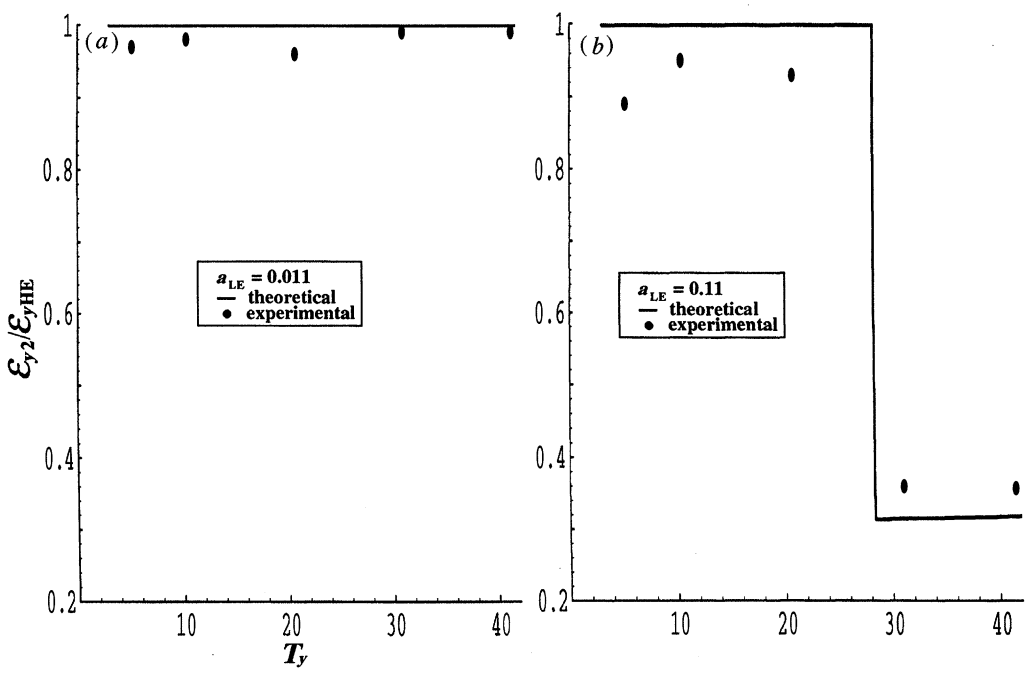

Figure 6. Comparisons between the secondary breaking strain of a hybrid composite and the breaking strain of the HE fibre composite. $\epsilon_{y2}/\epsilon_{y\mathrm{HE}}$ versus the twist factor T_{y} when: (*a*) $a_{\mathrm{LE}} = 0.011$; (*b*) $a_{\mathrm{LE}} = 0.11$.

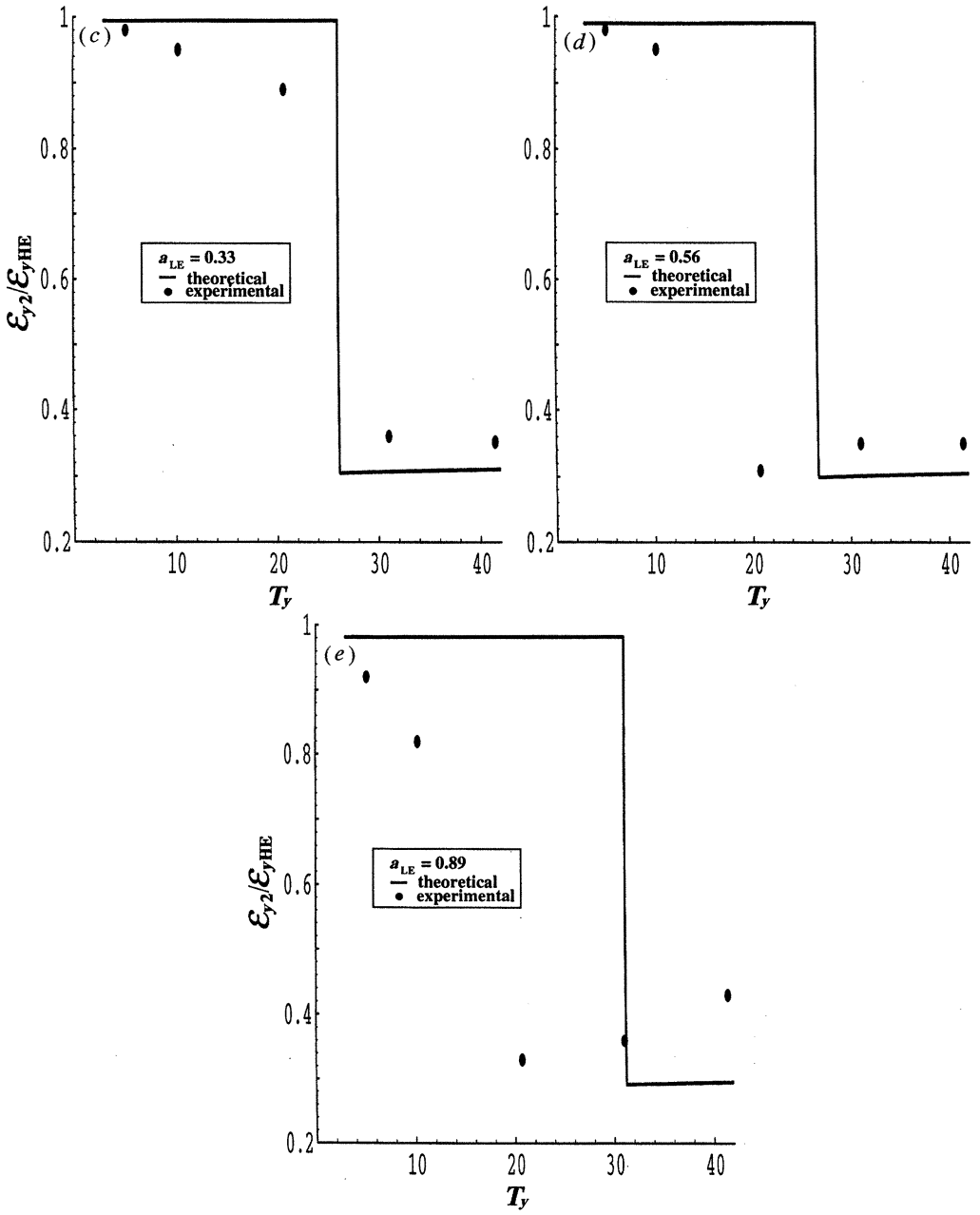

Figure 6. *Cont.* Comparisons between the secondary breaking strain of a hybrid composite and the breaking strain of the HE fibre composite. $\epsilon_{y2}/\epsilon_{y\mathrm{HE}}$ versus the twist factor T_{y} when: (*c*) $a_{\mathrm{LE}} = 0.33$; (*d*) $a_{\mathrm{LE}} = 0.56$; (*e*) $a_{\mathrm{LE}} = 0.89$.

the T_{y} value, $\epsilon_{y1}/\epsilon_{y\mathrm{LE}}$ drops abruptly to a level close to 1, and then further increase of a_{LE} only slightly reduces $\epsilon_{y1}/\epsilon_{y\mathrm{LE}}$. Overall, there exists a good agreement between the predicted and the experimental results from figures 3*a*–*e*.

It is also shown here that when T_{y} is beyond a certain level, $T_{\mathrm{y}} \geqslant 20.77$ in the present case, there appear oscillations in the predicted curves, similar to that reported in hybrid composites (Pan & Postle 1996). This is, however, not reflected by the

experimental results, very likely due to the fact that the resolution of the experiments is not as high as that of the theory. It should be pointed out that, although all the original functions involved in equation (3.1) are continuous, their derivatives may not necessarily also be continuous. The physical explanation for the oscillations in the figures is that, as the difference between LE and HE breaking strains in a hybrid structure is below a certain level, we will only see one stress-maximum (or peak) on the stress–strain curve associated with LE fibre type. Yet if we increase the difference high enough, the single peak splits into two, corresponding to two fibre types. Since this splitting of peak occurs over a very narrow strain range, takes place abruptly, and is therefore unstable in nature, one should not be too surprised to see the discontinuities in these figures.

The same investigation is done on the ratio $\epsilon_{y2}/\epsilon_{y\mathrm{HE}}$ and results can be seen in figure 4*a*–*e*, again for the same five different T_{y} levels. The ratio $\epsilon_{y2}/\epsilon_{y\mathrm{HE}}$ in all cases are no greater than 1, and the effects of a_{LE} is dependent on the twist level T_{y}. In figure 4, the ratio $\epsilon_{y2}/\epsilon_{y\mathrm{HE}} = 1$ when $a_{\mathrm{LE}} = 0$, so that the hybrid structure actually becomes a non-hybrid structure of HE component type and therefore $\epsilon_{y2} = \epsilon_{y\mathrm{HE}}$. First, in the case of low twist level when $T_{\mathrm{y}} \leqslant 20.77$, as a_{LE} increases, $\epsilon_{y2}/\epsilon_{y\mathrm{HE}}$ slightly decreases and then suddenly falls to a small value determined by the twist level when a_{LE} approaches a critical point very close to 1. Then, in the high twist case, where $T_{\mathrm{y}} \geqslant 31.10$, the critical value of a_{LE} at which $\epsilon_{y2}/\epsilon_{y\mathrm{HE}}$ plunges to a low level becomes much smaller. In other words, at the high twist level case, the breaking strain $\epsilon_{y\mathrm{HE}}$ is heavily influenced by the LE component so that the hybrid strand behaves more like a composite made of the LE component alone. That is, the structure becomes much more brittle with small breaking strain at high twist level, a result consistent with the conclusion in Monego *et al.* (1994). Furthermore, in all the above cases, good consistency is found between the theoretical and experimental results, except one case in figure 4*c* where the twist factor, $T_{\mathrm{y}} = 20.77$, is in the intermediate level. The theoretical model predicted a typical low twist behaviour, whereas the experimental data indicate a pattern of high twist case.

To better illustrate the influence of twist factor T_{y}, theoretical predictions are done focusing on the relationship between the breaking strain ratios and the twist factor at a given a_{LE} level.

The results for $\epsilon_{y1}/\epsilon_{y\mathrm{LE}}$ in comparison with the experimental data from table 2 are depicted in figure 5. In general, $\epsilon_{y1}/\epsilon_{y\mathrm{LE}}$ reduces as T_{y} increases at every level of a_{LE} from figure 5*a*–*e*. However, when the hybrid fraction a_{LE} is extremely small, as in figure 5*a* where $a_{\mathrm{LE}} = 0.011$, meaning that the hybrid composite is virtually made of the HE components only, the hybrid structure hence behaves more like a non-hybrid structure of HE components initially, and then gradually becomes less HE-type-like, reflected by a decreasing $\epsilon_{y1}/\epsilon_{y\mathrm{LE}}$ ratio as the twist level T_{y} goes up. Abruptly, $\epsilon_{y1}/\epsilon_{y\mathrm{LE}}$ falls off to a low level when T_{y} reaches a pivotal point. No such sudden changes occur at higher a_{LE} levels in figure 5*b*–*e*. In these later cases, a similar pattern is observed, and a_{LE} only influences the slope of the curves. Again, a reasonably good agreement between the predictions and the experimental data is seen in all the cases, except in figure 5*a* where the abrupt drop of the $\epsilon_{y1}/\epsilon_{y\mathrm{LE}}$ ratio is not reflected by the experimental results, which might be attributed to experimental errors.

The relationships between $\epsilon_{y2}/\epsilon_{y\mathrm{HE}}$ and T_{y}, both predicted and experimental, are illustrated in figure 6 at different hybrid fraction a_{LE} levels. Again, when the hybrid fraction is very small $a_{\mathrm{LE}} = 0.011$ in figure 6*a*, and the strand can be considered

as a non-hybrid strand of HE component so that $\epsilon_{y2}/\epsilon_{y\mathrm{HE}}$ is equal to 1, and seems independent of the twist level T_{y}. Yet when the hybrid fraction increases beyond $a_{\mathrm{LE}} = 0.11$, the curves become very different and consist of two portions. At low twist level, as twist increases, $\epsilon_{y2}/\epsilon_{y\mathrm{HE}}$ stays close to 1. However, once the twist level exceeds a critical level, $\epsilon_{y2}/\epsilon_{y\mathrm{HE}}$ drops sharply to a much small level whose value appears to be independent of the hybrid fraction a_{LE}. Then for further increase of twist, $\epsilon_{y2}/\epsilon_{y\mathrm{HE}}$ rises slightly. Although it shows that there exists a connection between this critical twist level and the hybrid fraction a_{LE}, the relation is not monotonic: the critical twist is the greatest when $a_{\mathrm{LE}} = 0.89$, followed by that when $a_{\mathrm{LE}} = 0.11$, then that of $a_{\mathrm{LE}} = 0.56$, and finally of $a_{\mathrm{LE}} = 0.33$. There is also a fair agreement between the theoretical predictions and the experimental results.

It should be pointed out that even though the present case focuses on a hybrid structure, this 'twist-bonding equivalence' principle is obviously also applicable to the study of non-hybrid composites.

Finally, although the present analysis, as well as several previous studies, has demonstrated the feasibility and advantages of using twisted yarn as a model to study composite behaviour, there are some limitations in this technique. First, the stress transfer mechanism in a yarn is through fibre–fibre friction, which may not be analogous in every aspect to a chemical bonding between fibre and matrix in a composite. Second, as seen from figure 1, there is an optimal value on the curve of the 'twist-bonding equivalence'. In other words, there is an upper limit in simulating the fibre–matrix bonding strength through a twisted strand, although this limit is found to cover most of the practical range of fibre–matrix bonding for real composites (Kelly & Macmillan 1986, p.263). So for a composite with extremely high relative bonding strength $\tau_{\mathrm{y}}/E_{\mathrm{f}}$, there may not be an equivalent yarn model for analysis. Third, when there is fibre breakage, the nature of load sharing by other surviving fibres is slightly different for the two cases. In a composite, this load sharing happens more locally than in a yarn.

5. Conclusions

The theories we developed in our previous paper have predicted some new and interesting results in hybrid composite behaviour. However, it is nearly impossible to verify most of the predictions experimentally because of the extreme difficulty in preparing hybrid composite samples whose properties can be reasonably well controlled. The main contribution in our present paper is that we suggest an approach to solve the problem, that is, to use twisted fibrous strictures, which are much easier to prepare with much less defects, and whose properties can be readily monitored, as samples for experiments. Then, by comparing the experiment results and theoretical predictions based on these twisted strands, our theories can be validated. Although the original theories are developed for hybrid composites, we can still use them for hybrid strands, owing to the 'twist-bonding equivalence' principle we proposed in this paper.

The feasibility of this technique has been demonstrated by the close agreement between the experimental results of the hybrid effect of breaking strains, and the corresponding theoretical predictions by the model developed for a hybrid composite but applied to the strands by substituting the strand parameters into the model.

According to the present analysis, there are two important variables controlling the fracture behaviour and the hybrid effects in a hybrid yarn, i.e. the hybrid fraction a_{LE}

for the LE component, and the twist factor T_y which is equivalent to the fibre–matrix bonding strength in a composite. When the a_{LE} value is small depending on the T_y level, there is always a positive hybrid effect in terms of breaking strains associated with the principal peak, and no noticeable hybrid effect with the secondary peak. As the a_{LE} value increases, however, beyond a critical level which is again related to the twist factor T_y, this positive hybrid effect at the principal peak diminishes, while a significant negative hybrid effect appears at the secondary peak.

There are limitations of this technique due to the different nature of 'fibre–matrix cohesion' in the two structures of fibre reinforced composite and strand.

References

Andersons, J. & Tamuzs, V. 1993 Fibre and interface strength distribution studies with the single-fibre composite test. *Composites Sci. Technol* **48**, 57.

Andrews, M. C. & Young, R. J. 1995 Fragmentation of aramid fibres in single-fibre model composites. *J. Mater. Sci.* **30**, 5607.

Aveston, J., Cooper, G. A. & Kelly, A. 1971 Single and multiple fracture: the properties of fibre composites. Conference Proceedings, National Physical Laboratory, Guildford, UK. *The properties of fibre composites*, pp. 15, Teddington: IPC Science and Technology Press.

Bader, M. G. & Manders, P. W. 1981 The strength of hybrid glass–carbon fibre composites. I. Failure strain enhancement and failure mode. *J. Mater. Sci.* **16**, 2233.

Baxevanakis, C., Jeulin, D. & Valentin, D. 1993 Fracture statistics of single-fibre composite specimens. *Composites Sci. Technol.* **48**, 47.

Bunsell, A. R. & Harris, B. 1974 Hybrid carbon and glass fibre composites. *Composites* **5**, 157.

Curtin, W. A. 1991 Exact theory of fibre fragmentation in a single-filament composite. *J. Mater. Sci.* **26**, 5239.

Curtin, W. A. 1991 Fibre fragmentation in a single-filament composite. *Appl. Phys. Lett.* **58**, 1155.

Curtin, W. A., Netravali, A. N. & Park, J. M. 194 Strength distribution of carborundum polycrystalline sic fibres as derived from the single-fibre-composite test. *J. Mater. Sci.* **29**, 4718.

Fariborz, S. J., Yang, C. L. & Harlow, D. G. 1985 The tensile behaviour of intraply hybrid composites. I. Model and simulation. *J. Comp. Mater.* **19**, 334.

Feillard, P., Desarmot, G. & Favre, J. P. 1994 Theoretical aspects of the fragmentation test. *Comp. Sci. Tech.* **50**, 265.

Fukuda, H., Chou, T. W, Schulte, K. & Peters, P. W. M. 1984 Probabilistic initial failure strength of hybrid and non-hybrid laminates. *J. Mater. Sci.* **19**, 974.

Fukunaga, H. & Chou, T. W. 1984 Probabilistic initial failure strength of hybrid and non-hybrid laminates. *J. Composite Mater.* **18**, 3546.

Goda, K., Park, J. M. & Netravali, A. N. 1995 A new theory to obtain Weibull fibre strength parameters from a single-fibre composite test. *J. Mater. Sci.* **30**, 2722–2728.

Harlow, D. G. 1983 Statistical properties of hybrid composites. I. Recursion analysis. *Proc. R. Soc. Lond.* A **389**, 67.

Hearle, J. W. S., Grosberg, P. & Backer, S. 1969 *Structural mechanics of yarns and fabrics*, vol. 1, p. 180. New York: Wiley-Interscience.

Ho, A., Netravali, A. N. & Phoenix, S. L. 1995 Interfacial shear strength studies of nicalon fibres in epoxy matrix using single fibre composite test. *Polymer Composites* **16**, 542.

Houpert J. L., Phoenix, S. L. & Raj, R. 1994 Analysis of the single-fibre-composite test to measure the mechanical properties of metal ceramic interfaces. *Acta Metal. Mater.* **42**, 4177.

Hsueh, C. H. 1992 Interfacial debonding and fibre pull-out stresses of fibre-reinforced composites. 8. The energy-based debonding criterion. *Mater. Sci. Engng* A **159**, 65.

Karbhari, V. M. & Engineer, M. 1995 Assessment of interfacial fracture energy between concrete and glass reinforced composites. *J. Mater. Sci. Lett.* **14**, 1210.

Kelly, A. & Macmillan, N. H. 1986 In *Strong solids*, 3rd edn, p. 252. Oxford: Clarendon.

Kodokian, G. K. A. & Kinloch, A. J. 1989 The adhesive fracture energy of bonded thermoplastic fibre-composites. *J. Adhesion* **29**, 193.

Kushnevsk, Y. V., Wacker, G. & Chate, A. 1994 The effect of interphase on residual thermal Stresses. 1. Single fibre composite materials. *Mech. Composite Mater.* **30**, 417.

Machida, K. 1963 Mechanics of rupture in blended yarns. M.S. thesis, MIT.

Manders, P. W. & Bader, M. G. 1981 The strength of hybrid glass–carbon fibre composites. I. Failure strain enhancement and failure mode. *J. Mater. Sci.* **16**, 2233.

Marom, G., Fischer, S., Tuler, F. R. & Wagner, H. D. 1978 Hybrid effects in composites: conditions for positive or negative effects versus rule of mixtures. *J. Mater. Sci.* **13**, 1419.

Monego, C. J. 1966 The mechanics of rupture of cotton-dacron yarns. M.S. thesis, MIT.

Monego, C. J. & Backer, S. 1968 Tensile rupture of blended yarns. *Textile Res. J.* **38**, 762.

Monego, C. J., Backer, S., Qui, Y. P. & Machida, K. 1994 Illustration of stress–strain behaviour and yarn fragmentation in a pseudo-hybrid composite system. *Composite Sci. Technol.* **50**, 451.

Netravali, A. N., Schwartz, P. & Phoenix, S. L. 1989 Study of interfaces of high-performance glass fibres and dgeba-based epoxy resins using single-fibre-composite test. *Polymer Composites* **10**, 385.

Pan, N. 1992 Development of a constitutive theory for short fibre yarns. I. Mechanics of staple yarn without slippage effect. *Textile Res. J.* **62**, 749.

Pan, N. 1993*a* Prediction of statistical strengths of twisted fibre structures. *J. Mater. Sci.* **28**, 6107.

Pan, N. 1993*b* Theoretical determination of the optimal fiber volume fraction and fibre–matrix property compatibility for short fibre reinforced composites. *Polymer Composites* **14**, 85.

Pan, N. & Postle, R. 1996 Tensile strengths and the hybrid effects of hybrid fibre composites: a probabilistic approach. *Trans. R. Soc. Lond.* A 354, 1875.

Park, J. M., Subramanian R. V. & Bayoumi, A. E. 1994 Interfacial shear strength and durability improvement by silanes in single-filament composite specimens of basalt fibre in brittle phenolic and isocyanate resins. *J. Adhesion Sci. Technol.* **8**, 133.

Phillips, L. N. 1976 Hybrid effect. Does it exist? *Composites* **7**, 7.

Phoenix, S. L. 1979*a* Statistical theory for the strength of twisted fibre bundles with applications to yarns and cables. *Textile Res. J.* **49**, 407–423.

Phoenix, S. L. 1979*b* Statistical aspects of failure of fibrous materials. *Composite materials: testing and design (5th Conf.), ASTM STEP 674* (ed. S. W. Tsai), pp. 407–423, 455.

Pitt, R. E. & Phoenix, S. L. 1981 On modelling the statistical strength of yarns and cables under localized load-sharing among fibres. *Textile Res. J.* **51**, 408.

Qiu, Y. P. & Schwartz, P. 1993 Micromechanical behaviour of kevlar-149/S–glass hybrid seven-fibre microcomposites. I. Tensile strength of the hybrid composite. *Composites Sci. Technol.* **47**, 289.

Shioya, M. & Takaku, A. 1995 Estimation of fibre and interfacial shear strength by using a single-fibre composite. *Composite Sci. Technol.* **55**, 33.

Venkatakrishnaiah, S. & Dharani, L. R. 1993 Analysis of an axisymmetric matrix crack in a single fibre composite. *Eur. J. Mech.* A **12**, 567.

Wagner, H. D. & Eitan, A. 1990 Interpretation of the fragmentation phenomenon in single-filament composite experiments. *Appl. Phys. Lett.* **56**, 1965.

Wagner, H. D., Rubins, M. & Marom, G. 1991 The significance of microcomposites as experimental models. *Polymer Composites* **12**, 233.

Watson, M. C. & Clyne, T. W. 1992 The use of single fibre pushout testing to explore interfacial mechanics in sic monofilament-reinforced Ti. 2. Application of the test to composite material. *Acta Metall. Mater.* **40**, 141.

Yavin, B., Gallis, H. E., Scherf, J., Eitan, A. & Wagner, H. D. 1991 Continuous monitoring of the fragmentation phenomenon in single fibre composite materials. *Polymer Composites* **12**, 436.

Zweben, C. 1977 Tensile strength of hybrid composites. *J. Mater. Sci.* **12**, 1325.